The Astrophysical Journal, 689:613–621, 2008 December 10

THE DISTRIBUTION, EXCITATION, AND FORMATION OF COMETARY MOLECULES: METHANOL, METHYL CYANIDE, AND ETHYLENE GLYCOL

Anthony J. Remijan,[1] Stefanie N. Milam,[2,3] Maria Womack,[4] A. J. Apponi,[2] L. M. Ziurys,[2] Susan Wyckoff,[5] M. F. A'Hearn,[6] Imke de Pater,[7] J. R. Forster,[7] D. N. Friedel,[8] Patrick Palmer,[9] L. E. Snyder,[8] J. M. Veal,[8,10] L. M. Woodney,[11] and M. C. H. Wright[7]

Received 2008 July 3; accepted 2008 July 23

ABSTRACT

We present an interferometric and single-dish study of small organic species toward Comets C/1995 O1 (Hale-Bopp) and C/2002 T7 (LINEAR) using the BIMA interferometer at 3 mm and the ARO 12 m telescope at 2 mm. For Comet Hale-Bopp, both the single-dish and interferometer observations of CH_3OH indicate an excitation temperature of 105 ± 5 K and an average production rate ratio $Q(CH_3OH)/Q(H_2O) \sim 1.3\%$ at $\sim$1 AU. In addition, the aperture synthesis observations of CH_3OH suggest a distribution well described by a spherical outflow and no evidence of significant extended emission. Single-dish observations of CH_3CN in Comet Hale-Bopp indicate an excitation temperature of 200 ± 10 K and a production rate ratio of $Q(CH_3CN)/Q(H_2O) \sim 0.017\%$ at $\sim$1 AU. The nondetection of a previously claimed transition of cometary $(CH_2OH)_2$ toward Comet Hale-Bopp with the 12 m telescope indicates a compact distribution of emission, $D < 9''$ (<8500 km). For the single-dish observations of Comet T7 LINEAR, we find an excitation temperature of CH_3OH of 35 ± 5 K and a CH_3OH production rate ratio of $Q(CH_3OH)/Q(H_2O) \sim 1.5\%$ at $\sim$0.3 AU. Our data support current chemical models that CH_3OH, CH_3CN, and $(CH_2OH)_2$ are parent nuclear species distributed into the coma via direct sublimation off cometary ices from the nucleus with no evidence of significant production in the outer coma.

Subject headings: astrobiology — comets: individual (Hale Bopp [C/1995 01], LINEAR [C/2002 T7]) — molecular processes — radio lines: solar system — techniques: interferometric

1. INTRODUCTION

Over the last several years, complementary observations of comets with both single-dish telescopes and interferometric arrays have shed new light on the abundance, production rate, distribution, and formation of molecules in cometary comae. Recently, Milam et al. (2006) employed this method to investigate the origins of cometary formaldehyde (H_2CO) by comparing observations with both the Arizona Radio Observatory (ARO) 12 m[12] single-dish telescope and the Berkeley-Illinois-Maryland Association (BIMA) array.[13] From this investigation toward Comet C/1995 O1 (Hale-Bopp), the authors clearly showed that the distribution and abundance of H_2CO must be coming from a source other than the comet nucleus. The extended source of H_2CO may be due to enhanced production of this molecule ($\sim$4 times larger) from grains consisting of silicates and organic material (Milam et al. 2006), or possibly from the photodissociation of a larger parent species such as methanol (CH_3OH; Hudson et al. 2005). These complementary observations, however, are very difficult to obtain, as most of the molecular observations toward comets are performed using solely single-dish telescopes or interferometric arrays, depending on the telescope available at the time as the comet approaches the inner solar system and perigee.

Multiple facility collaborations for cometary observations are necessary if we are to further understand the formation, excitation, and distribution of organic cometary material. Recent cometary models of the abundance of organic material suggest Oort Cloud comets may have had their origin in the giant planet region, where they were thermally and chemically processed, before being ejected into the Oort Cloud (Weissman 1999). Furthermore, observations comparing long- and short-period comets suggest distinct classes: organic "rich," "normal," and "depleted" (Bonev et al. 2008; Mumma et al. 2003). However, the current sample size is too limited to accurately characterize each class of comets. It should also be noted that many of the comets described as organic "rich" have undergone breakup or fragmentation events, thus exposing more internal, unprocessed material than an object just entering the inner solar system (Bonev et al. 2008). So, the question persists, how does the classification of organic "rich," "normal," or "depleted" hold with regard to comets that, for example, are dust-rich versus dust-poor, have undergone a recent breakup, or bear high abundances of hypervolatile species?

The organic species examined in this study, methanol (CH_3OH), methyl cyanide (CH_3CN), and ethylene glycol [$(CH_2OH)_2$], are believed to be parent species directly sublimated off the cometary

[1] National Radio Astronomy Observatory, 520 Edgemont Road, Charlottesville, VA 22901; aremijan@nrao.edu.
[2] NASA Astrobiology Institute, Department of Chemistry, Department of Astronomy, and Steward Observatory, University of Arizona, 933 North Cherry Avenue, Tucson, AZ 85721; lziurys@as.arizona.edu, aapponi@as.arizona.edu.
[3] Current address: NASA Ames Research Center, Astrophysics Branch, MS 245-6, Moffett Field, CA 94035-1000; stefanie.n.milam@nasa.gov.
[4] Department of Physics and Astronomy, St. Cloud State University, St. Cloud, MN 56301; mwomack@stcloudstate.edu.
[5] Department of Physics and Astronomy, Arizona State University, Tempe, AZ 85287; wyckoff@asu.edu.
[6] Department of Astronomy, University of Maryland, College Park, MD 20742-2421; ma@astro.umd.edu.
[7] Department of Astronomy, University of California, Berkeley, CA 94720; imke@floris.berkeley.edu, rforster@astro.berkeley.edu, wright@astro.berkeley.edu.
[8] Department of Astronomy, University of Illinois, 1002 West Green Street, Urbana, IL 61801; friedel@astro.uiuc.edu, snyder@astro.uiuc.edu.
[9] Department of Astronomy and Astrophysics, University of Chicago, Chicago, IL 60637; ppalmer@oskar.uchicago.edu.
[10] Current address: Southwestern College, 900 Otay Lakes Road, Chula Vista, CA 91910; jveal@swccd.edu.
[11] Department of Physics, California State University, San Bernardino, CA 92407; woodney@csusb.edu.
[12] The Kitt Peak 12 m telescope is currently operated by ARO, Steward Observatory, University of Arizona.
[13] Operated by the University of California, Berkeley, the University of Illinois, and the University of Maryland with support from the National Science Foundation.

TABLE 1
CH_3OH Observational Parameters: BIMA Array

Frequency (GHz)	Observation Date (UT)	Δ (AU)	r (AU)	Beam	Channel rms (Jy beam^{-1})
96.741.....	1997 Mar 27	1.323	0.919	10.8 × 8.2	0.21
	1997 Mar 31	1.344	0.914	9.8 × 7.8	0.20
107.014.....	1997 Mar 26	1.320	0.921	19.3 × 6.8	0.43
	1997 Apr 2	1.359	0.914	11.7 × 6.6	0.15
	1997 Apr 3	1.367	0.915	16.0 × 6.4	0.30

ices in the nucleus. Since the first reported single-dish detections of cometary CH_3OH toward Comet Brorsen-Metcalf (1989 o) and Comet Austin (1989 c1) (Colom et al. 1990), CH_3OH remains the most abundant large (>5 atoms) organic (containing a C atom) molecule measured in cometary ices. In a recent review by Charnley & Rodgers (2008), CH_3OH has a measured abundance range relative to H_2O between 1% and 4%. However, aperture synthesis observations of cometary CH_3OH are very rare, and no high spatial resolution data of this molecule currently exist. Similarly, single-dish observations of CH_3CN and $(CH_2OH)_2$ also suggest a purely nuclear origin (Biver et al. 2002; Crovisier et al. 2004). CH_3CN and HC_3N may be parent species that would increase the abundance of the CN radical, as well as C_2 in the coma. Yet, current observations do not preclude the possibility of CH_3CN having its own parent species (Bockelée-Morvan et al. 1987). In addition, the high abundance of $(CH_2OH)_2$ observed in Comet Hale-Bopp at high spatial resolution also strongly suggests a nuclear origin. To date, complementary observations of the same transitions of either CH_3CN or $(CH_2OH)_2$ with another facility were not available to follow up on the claimed distribution of these species in the coma and their possible formation pathways.

In this paper, we report on complementary observations of cometary CH_3OH, CH_3CN, and $(CH_2OH)_2$ taken with the BIMA array near Hat Creek, California, and the ARO 12 m telescope on Kitt Peak, Arizona, toward Comets C/1995 O1 (Hale-Bopp) and C/2002 T7 (LINEAR). From these observations, we continued to investigate the abundance, production rate, distribution, and formation of molecules in comets by directly comparing the measurements of these organic species with different telescopes. Our data support the hypothesis that CH_3OH, CH_3CN, and $(CH_2OH)_2$ are primarily parent species, generated by direct sublimation of cometary ices contained in the nucleus.

2. OBSERVATIONS

2.1. *BIMA Array*

Our observations of Comet Hale-Bopp with the BIMA array constitute one of the earliest detections of cometary CH_3OH with an interferometer. These measurements were taken using the "soft" C configuration of the BIMA array from 1997 March 24 to April 3. Data were acquired in the interferometric (cross-correlation) mode with nine antennas. The minimum baseline for these observations was ∼15 m, and the maximum baseline was ∼139 m. The average resulting full width at half-power synthesized beam size was $\sim 8'' \times 10''$ for the observations. The quasar 0102+584 was used to calibrate the antenna-based gains, and the absolute amplitude calibration of this source was based on planetary observations and is accurate to within ∼20%. The spectral windows containing the transitions had a bandwidth of 25 MHz and were divided into 256 channels for a spectral resolution of 0.1 MHz per channel. However, to increase the signal-to-noise ratio (S/N) in each window, the data were averaged over two channels, giving an effective spectral resolution of 0.2 MHz per channel. All data were first corrected to JPL ephemeris reference orbit 139. The data were then combined and imaged using the MIRIAD software package (Sault et al. 1995). To include all the data from the comet with multiple tracks, the data were inverted in u-v space. The resulting synthesized beam size was determined from the combined data set. The u-v data from multiple tracks were combined to make images. Table 1 summarizes the observational parameters of the BIMA array observations.

2.2. 12 m *Single Dish*

Observations at 2 mm of CH_3OH, CH_3CN, and $(CH_2OH)_2$ toward Comet Hale-Bopp were taken during three observing runs on 1997 March 10, 11, and 20 using the ARO (at the time, NRAO)[14] 12 m telescope. Observations of CH_3OH toward Comet LINEAR were conducted on 2004 May 20, also using the ARO 12 m telescope. Dual-channel SIS mixers were used for the 2 mm observations, operated in single-sideband mode with ∼20 dB image rejection. The back ends employed for the presented observations were individual filter banks with 500 kHz resolution and the millimeter autocorrelator (MAC) with a resolution of 781 kHz. The spectral temperature scale was determined by the chopper-wheel method, corrected for forward spillover losses, and given in terms of T_R^* (K). The radiation temperature, T_R, is then derived from the corrected beam efficiency, η_c, where $T_R = T_R^*/\eta_c$. A two-body ephemeris program was used to determine the comet's position using the orbital elements provided by D. Yeomans (1996, private communication) of JPL for Comet Hale-Bopp, and JPL ephemeris reference orbit 69 was used for the Comet LINEAR observations. Focus and positional accuracy were checked periodically on nearby planets or maser sources. Data were taken in the position-switched mode with the off position 30′ west in azimuth. Observing frequencies, dates, comet geocentric and heliocentric distances, beam size, the diameter of the projected beam size on the comet, and the corrected main beam efficiency (η_c) at the times of observation are listed in Table 2.

Table 3 lists the transitions and molecular line parameters of CH_3OH, CH_3CN, and $(CH_2OH)_2$. All spectral line data were taken from the Spectral Line Atlas of Interstellar Molecules (SLAIM)[15] (Remijan et al. 2007) and the Cologne Database for Molecular Spectroscopy (Müller et al. 2005).

3. RESULTS

3.1. *BIMA Array*

Figure 1 shows the images and spectra of CH_3OH taken toward Comet Hale-Bopp with the BIMA array. Figure 1*a* shows

[14] The National Radio Astronomy Observatory is a facility of the National Science Foundation operated under cooperative agreement by Associated Universities, Inc.

[15] Available at http://www.splatalogue.net.

TABLE 2
OBSERVATIONAL PARAMETERS: ARO 12 m

Frequency (GHz)	Observation Date (UT)	Δ (AU)	r (AU)	Beam (arcsec)	D (km)	η_c	Molecule
			Comet Hale-Bopp				
145.766.....	1997 Mar 20.94	1.318	0.940	43	41105	0.76	CH_3OH
147.105[a].....	1997 Mar 20.66	1.318	0.940	43	41105	0.76	CH_3CN
148.112.....	1997 Mar 11.89	1.368	0.989	42	41672	0.76	CH_3OH
150.142.....	1997 Mar 10.71	1.377	0.996	42	41946	0.75	CH_3OH
151.860.....	1997 Mar 20.92	1.318	0.940	41	39193	0.74	CH_3OH
157.049.....	1997 Mar 21.54	1.316	0.936	40	38179	0.72	CH_3OH
			Comet LINEAR				
157.261[b].....	2004 May 21.80	0.284	0.865	40	8239	0.72	CH_3OH

[a] Average of observing frequencies between the $K = 7$ and $K = 0$ lines of CH_3CN.
[b] Average of observing frequencies of CH_3OH lines detected in the same spectral passband.

the image of the $J(K_a, K_c) = 2(0, 2)$–$1(0, 1)$ E transition of CH_3OH averaged over 2 days, 1997 March 27 and 31. Note that the CH_3OH emission is slightly larger than the synthesized beam of the BIMA array (located at the bottom left of each image) and follows the general position angle of the synthesized beam. The projected direction to the Sun is shown by the line segment. The coordinates are given in offset arcseconds centered on the comet nucleus. Figure 1*b* shows the spectra of four CH_3OH transitions near 96.7 GHz (Table 3), including the $J(K_a, K_c) = 2(0, 2)$–$1(0, 1)$ E transition. The spectrum has been Hanning smoothed over three channels. The rms noise level is $\sim$0.1 Jy beam^{-1} (indicated by the vertical bar at the left of the spectrum). The spectral line labels correspond to the rest frequency located at the top left of the panel for a cometocentric velocity of 0 km s^{-1} (*dashed line*).

Figure 1*c* shows the image of the $J(K_a, K_c) = 3(1, 3)$–$4(0, 4)$ A^+ transition of CH_3OH averaged over 3 days, 1997 March 26 and April 2–3. Figure 1*d* shows the spectrum of this CH_3OH transition near 107.0 GHz (Table 3). Note that the two CH_3OH emission contours shown in Figures 1*a* and 1*c* are centered on the predicted location of the comet nucleus with no apparent offset. The images are similar to each other and to the average of the March HCN BIMA array contours given by Veal et al. (2000) and the CO BIMA array contours given by Milam et al. (2006). In addition, there is no pronounced evidence for the jets or significant extended enhancement of CH_3OH beyond the 3 σ detection level (§ 4.2). Furthermore, from Figures 1*b* and 1*d*, there is no apparent second velocity component of CH_3OH, nor is the emission offset from the cometocentric rest velocity of 0 km s^{-1}.

TABLE 3
MOLECULAR LINE PARAMETERS

Molecule (1)	Transition (2)	Frequency[a] (MHz) (3)	$\langle S_{i,j}\mu^2 \rangle$ (D^2) (4)	$A_{i,j}$ (s^{-1}) (5)	E_u (K) (6)
CH_3OH[b]	$J(K_a, K_c) = 2(-1, 2)$–$1(-1, 1)$ E	96,739.363(3)	1.2	2.55×10^{-6}	12.6
	2(0,2)–1(0,1) A^+	96,741.377(3)	1.6	3.41×10^{-6}	7.0
	2(0,2)–1(0,1) E	96,744.549(3)	1.6	3.41×10^{-6}	20.1
	2(1,1)–1(1,0) E	96,755.507(3)	1.2	2.62×10^{-6}	28.0
	3(1,3)–4(0,4) A^+	107,013.770(13)	3.0	6.13×10^{-6}	28.4
	16(0,16)–16(−1,16) E	145,766.163(27)	7.0	7.60×10^{-6}	327.9
	15(0,15)–15(−1,15) E	148,111.919(24)	7.3	8.80×10^{-6}	290.9
	14(0,14)–14(−1,14) E	150,141.593(22)	7.5	10.2×10^{-6}	256.3
	13(0,13)–13(−1,13) E	151,860.170(20)	7.6	11.5×10^{-6}	223.9
	6(0,6)–6(−1,6) E	157,048.586(13)	5.7	1.96×10^{-6}	61.9
	4(0,4)–4(−1,4) E	157,246.041(14)	4.2	21.0×10^{-6}	36.4
	1(0,1)–1(−1,1) E	157,270.818(15)	1.5	22.1×10^{-6}	15.5
	3(0,3)–3(−1,3) E	157,272.320(14)	3.3	21.5×10^{-6}	27.1
	2(0,2)–2(−1,2) E	157,276.004(14)	2.4	21.8×10^{-6}	20.1
CH_3CN[b]	$J(K) = 8(6)$–$7(6)$	147,072.608(2)	53.2	0.58×10^{-4}	289.0
	8(5)–7(5)	147,103.741(1)	74.2	1.62×10^{-4}	210.5
	8(4)–7(4)	147,129.232(1)	91.3	1.99×10^{-4}	146.2
	8(3)–7(3)	147,149.068(1)	104.6	1.14×10^{-4}	96.1
	8(2)–7(2)	147,163.243(1)	114.1	2.49×10^{-4}	60.4
	8(1)–7(1)	147,171.750(1)	119.8	2.61×10^{-4}	38.9
	8(0)–7(0)	147,174.587(1)	121.7	2.66×10^{-4}	31.8
$(CH_2OH)_2$[c]	$J(K_a, K_c, v) = 15(7, 9, 0)$–$14(7, 8, 1)$	147,131.814(36)	2.5	5.99×10^{-5}	83.1
	15(7,8,0)–14(7,7,1)	147,132.412(36)	2.7	5.99×10^{-5}	83.1

[a] Uncertainties in parentheses refer to the least significant digit and are 2 σ values (type A coverage; Taylor & Kuyatt 1994).
[b] Molecular line parameters of CH_3OH and CH_3CN taken from SLAIM; $Q_r = 1.2T_r^{3/2}$ for CH_3OH and $Q_r = 3.9T_r^{3/2}$ for CH_3CN.
[c] Molecular line parameters of $(CH_2OH)_2$ taken from CDMS (Müller et al. 2005). The energy levels are noted as $J(K_a, K_c, v)$, where v is the quantum number associated with OH tunneling (Christen & Müller 2003).

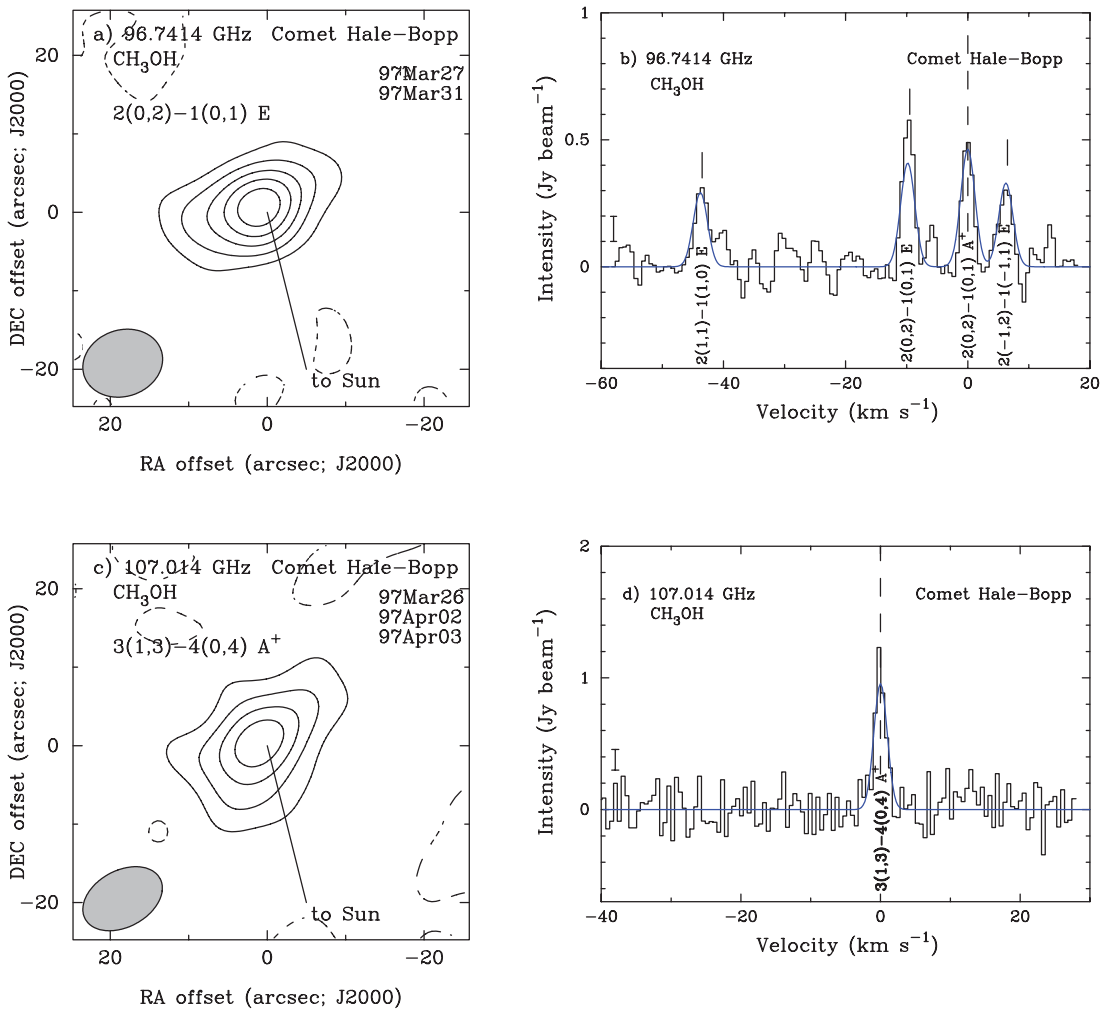

FIG. 1.—CH_3OH lines detected toward Comet Hale-Bopp with the BIMA array. (*a*) Emission contours from the 2(0,2)–1(0,1) *E* transition of CH_3OH at 96.741 GHz. Contours indicate the location of the 2(0,2)–1(0,1) *E* CH_3OH emission. The contour levels are −0.2, 0.4, 0.6, 0.8, 1.0, and 1.2 Jy beam^{-1}. The synthesized beam of $10.3'' \times 8.5''$ is indicated in the bottom left corner. (*b*) CH_3OH spectrum toward Comet Hale-Bopp (Hanning smoothed over three channels). The rms noise level is ~0.1 Jy beam^{-1} (*vertical bar at left*). The spectral line labels correspond to the rest frequency located at the top left of the spectral window for a velocity of 0 km s^{-1}. The dashed line is centered on this velocity. The blue line shows a model fit (see text). (*c*) Emission contours from the 3(1,3)–4(0,4) A^+ transition of CH_3OH at 107.014 GHz. Contours indicate the location of the CH_3OH emission averaged between −2 and 2 km s^{-1}. The contour levels are −0.05, 0.20, 0.30, 0.40, 0.50, and 0.60 Jy beam^{-1}. The synthesized beam of $10.8'' \times 7.2''$ is indicated in the bottom left corner. (*d*) CH_3OH spectrum toward Comet Hale-Bopp. The rms noise level is ~0.1 Jy beam^{-1} (*vertical bar at left*). The spectral line label is the same as in (*b*), and the blue line shows a model fit (see text).

3.2. 12 m *Single Dish*

Figure 2 shows the spectra of the five $\lambda \simeq 2$ mm transitions of CH_3OH detected toward Comet Hale-Bopp with the 12 m telescope (Table 3). The UT date and spectral line quantum numbers of each observed transition are located at the top of each panel. As in the BIMA spectra, the spectral line labels correspond to the rest frequency of that transition for a cometocentric velocity of 0 km s^{-1} (*dashed line*). The CH_3OH detections reported by the 12 m data are all *E*-type transitions. Similarly, Figure 3 shows the spectrum of a cluster of *E*-type transitions of CH_3OH centered around 157.3 GHz observed toward Comet LINEAR with the ARO 12 m telescope.

Finally, Figure 4 shows the spectrum taken at the frequency of the $J = 8$–7 ($K = 0$–7) transitions of the symmetric top species methyl cyanide (CH_3CN) toward Comet Hale-Bopp using the 12 m telescope. The $K = 0$–6 components are clearly present in these data. CH_3CN and other symmetric tops have properties that make them ideal probes of physical conditions of astronomical environments (see, e.g., Araya et al. 2005; Remijan et al. 2004; Hofner et al. 1996). As with CH_3OH, there are no apparent additional velocity components of CH_3CN or offset from the cometocentric rest velocity of 0 km s^{-1}.

Table 4 lists the molecular species that were searched for toward Comets Hale-Bopp and LINEAR at or near the cometocentric velocity (0 km s^{-1}). Least-squares Gaussian fits were made for each spectral line in order to obtain the peak intensities and line widths for the detected transitions. For those transitions not detected, the 1 σ rms noise level is given. The spectroscopic parameters used in determining the column densities and production rates are found in Table 3, and the formalism for calculating column densities and production rates is described in § 4.1.

4. ANALYSIS AND DISCUSSION

4.1. *Excitation, Abundances, and Production Rates*

Determining the best temperature, column density, and production rates of cometary molecules is important because these factors are essential to understanding the formation of cometary species. This includes the role of grains in molecule formation, the relative impact of warm versus cold gas-phase chemistry, or the importance of photodissociation in the production of daughter

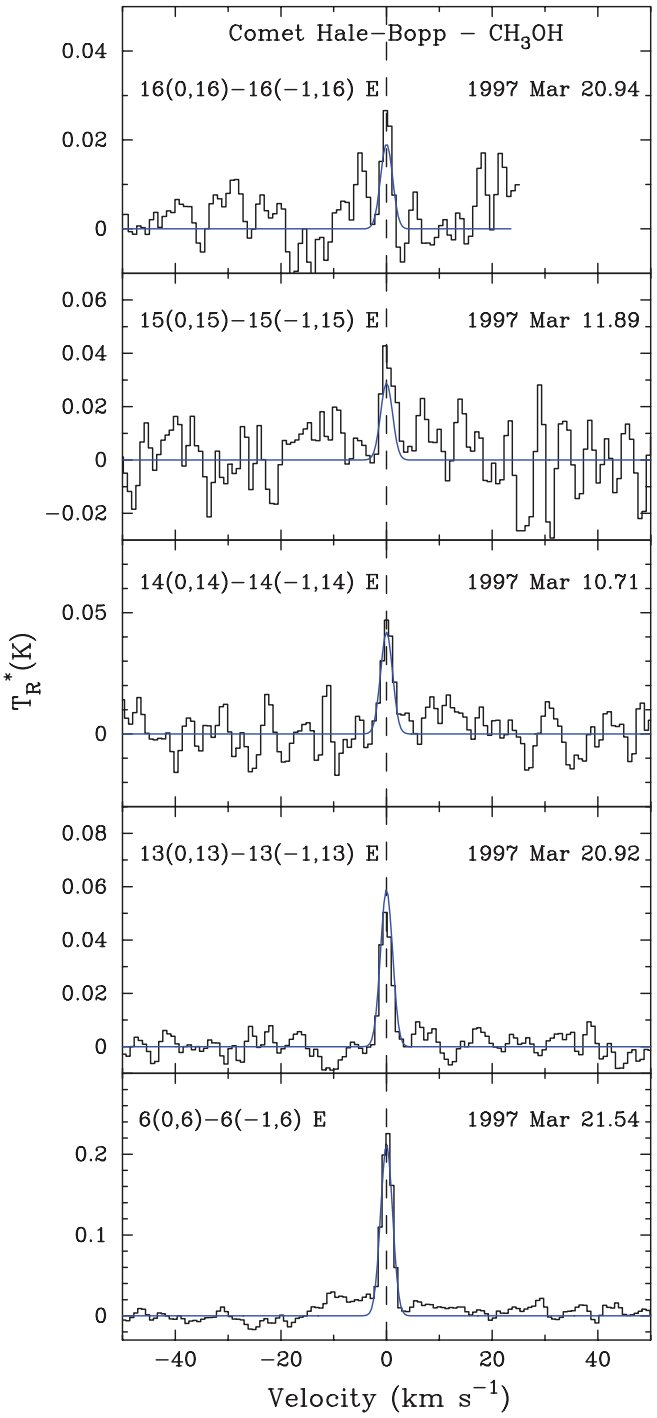

FIG. 2.—CH_3OH lines detected toward Comet Hale-Bopp with the 12 m telescope. The back ends employed for the presented observations were a MAC with a resolution of 781 kHz. The spectral line labels correspond to the rest frequency located at the top left of the spectral window for a velocity of 0 km s^{-1} (*dashed line*). The blue lines show a model fit (see text).

species in the coma. In order to determine the temperatures and column densities of the region of the coma that contains the CH_3OH and CH_3CN emission, we assume that each region has uniform physical conditions, that the populations of the energy levels can be characterized by a Boltzmann distribution, and finally, that the emission is optically thin. The rotational temperature diagram method was not employed for this analysis because even small errors in the intensities and widths of inherently weak spectral lines can cause large errors in determining the temperature and total column density (see, e.g., Snyder et al. 2005). The complete formalism for these calculations using the BIMA array data can be found in Remijan et al. (2006), and for the 12 m data it can be found in Milam et al. (2006).

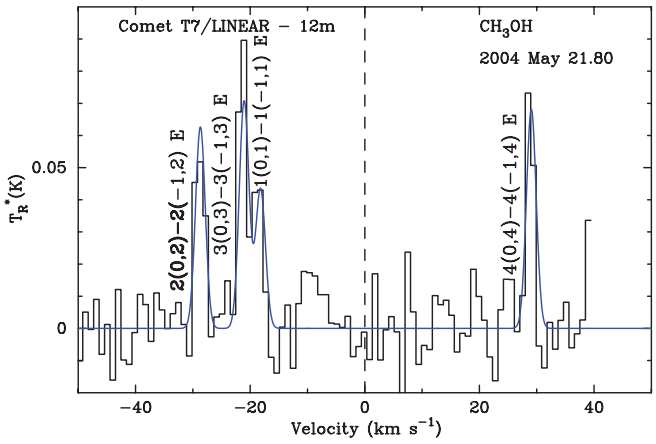

FIG. 3.—CH_3OH lines detected toward Comet LINEAR with the 12 m telescope. Spectral resolution is 500 kHz, and the spectral line labels are similar to those in Fig. 2. The blue line shows a model fit (see text).

Figure 1 shows the results of the model fit (*blue line*) applied to the CH_3OH BIMA array data toward Comet Hale-Bopp. The array data are well fit by an excitation temperature of $T_{ex} = 105 \pm 5$ K and a total beam-averaged column density of $N_T = (9 \pm 1) \times 10^{14}$ cm^{-2}, assuming that the CH_3OH emission is extended beyond the $10.33'' \times 8.46''$ average synthesized beam of the BIMA array (i.e., the beam filling factor, $f = 1$). Similarly, Figure 2 shows the results of the model fit applied to the CH_3OH ARO 12 m data with the same excitation temperature and a slightly lower column density of $N_T = (2.4 \pm 0.3) \times 10^{14}$ cm^{-2}. The average total column density from these two facilities is $N_T = (5.7 \pm 0.7) \times 10^{14}$ cm^{-2}. As the figure shows, the modeling reproduces the observations. Assuming that CH_3OH is a parent species, production rates were determined from a Monte Carlo model for a nuclear source (see Combi & Smyth 1988). This model traces the trajectories of molecules within the telescope beam ejected from the comet surface. The observed column density is then matched for an output molecular production rate, Q (s^{-1}). Input parameters include the lifetime of the molecule

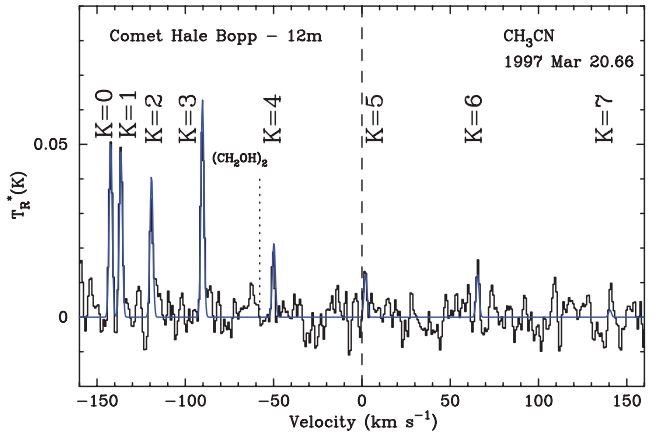

FIG. 4.—CH_3CN lines detected toward Comet Hale-Bopp with the 12 m telescope. Spectral resolution is 781 kHz, and the spectral line labels are similar to those in Fig. 2. The blue line shows the model fit (see text).

TABLE 4
COMET HALE-BOPP AND COMET LINEAR MOLECULAR LINE IDENTIFICATIONS

Species	Telescope	ν (MHz)	Transition	$I_{\rm line}$[a,b]	Δv[b] (km s^{-1})	N_T (cm^{-2})	Q_p (s^{-1})	Q_X/Q_{H_2O}
Comet Hale-Bopp								
CH_3OH	BIMA	96,739.4	2(−1,2)–1(−1,1) E	0.31(5)	2.4(2)	$(9 \pm 1) \times 10^{14}$	$(1.1 \pm 0.3) \times 10^{29}$	$\sim 1.1 \times 10^{-2}$[c]
		96,741.4	2(0,2)–1(0,1) A^+	0.52(5)	2.0(2)			
		96,744.5	2(0,2)–1(0,1) E	0.60(5)	2.1(2)			
		96,755.5	2(1,1)–1(1,0) E	0.29(5)	3.2(2)			
		107,013.8	3(1,3)–4(0,4) A^+	1.12(5)	1.9(2)			
CH_3OH	12 m	145,766.2	16(0,16)–16(−1,16) E	0.03(2)	2.0(8)	$(2.4 \pm 0.3) \times 10^{14}$	$(1.5 \pm 0.3) \times 10^{29}$	$\sim 1.5 \times 10^{-2}$
		148,111.9	15(0,15)–15(−1,15) E	0.04(2)	3.0(8)			
		150,141.6	14(0,13)–14(−1,14) E	0.04(1)	1.9(8)			
		151,860.2	13(0,13)–13(−1,13) E	0.05(1)	2.5(8)			
		157,048.6	6(0,6)–6(−1,6) E	0.23(1)	2.4(8)			
CH_3OH average						$(5.7 \pm 0.7) \times 10^{14}$	$(1.3 \pm 0.3) \times 10^{29}$	$\sim 1.3 \times 10^{-2}$
CH_3CN	12 m	147,129.2	8(4)–7(4)	0.019(1)	1.6(8)	$(2.6 \pm 0.3) \times 10^{12}$	$(1.7 \pm 0.3) \times 10^{27}$	$\sim 1.7 \times 10^{-4}$
		147,149.0	8(3)–7(3)	0.054(1)	2.8(8)			
		147,163.2	8(2)–7(2)	0.034(1)	3.2(8)			
		147,171.7	8(1)–7(1)	0.049(1)	2.4(8)			
		147,174.5	8(0)–7(0)	0.051(1)	2.4(8)			
$(CH_2OH)_2$	12 m	147,131.8	15(7,*,0)–14(7,*,0)[d]	<0.01				
Comet LINEAR								
CH_3OH	12 m	157,246.1	6(0,6)–6(−1,6) E	0.087(1)	1.9(10)	$(2.2 \pm 0.3) \times 10^{13}$	$(2.0 \pm 0.3) \times 10^{27}$	$\sim 1.5 \times 10^{-2}$[e]
		157,270.9	1(0,1)–1(−1,1) E	0.051(1)	1, 9(10)			
		157,272.3	3(0,3)–3(−1,3) E	0.101(1)	1, 9(10)			
		157,276.0	2(0,2)–2(−1,2) E	0.058(1)	1, 9(10)			

[a] For the BIMA data, $I_{\rm line}$ represents ΔI in units of Jy beam^{-1}. For the 12 m observations, $I_{\rm line}$ represents T_R^* in units of K.
[b] Uncertainties in parentheses refer to the least significant digit and are 2 σ values (type A coverage; Taylor & Kuyatt 1994).
[c] Comet Hale-Bopp: $Q(H_2O) = 10^{31}$ s^{-1} (Crovisier et al. 2004).
[d] The two $(CH_2OH)_2$ transitions are not resolved given the spectral resolution of our spectrometer passband. This is indicated by the asterisk substituted for the K_c quantum numbers. Frequencies and specific K_c values for these two transitions can be found in Table 3.
[e] Comet T7/LINEAR: $Q(H_2O) = 1.3 \times 10^{29}$ s^{-1} (Milam et al. 2006).

from Huebner et al. (1992) scaled by R_h^2, the outflow velocity, the telescope beam size, and the observed column density. Assuming a nuclear origin for CH_3OH and using this Monte Carlo model, we find an average CH_3OH production rate from both instruments of $Q(CH_3OH) \sim 1.3 \times 10^{29}$ s^{-1} or $Q(CH_3OH)/Q(H_2O) \sim 1.3\%$ at $\sim$1 AU. This production rate ratio assumes $Q(H_2O) = 10^{31}$ s^{-1} (Crovisier et al. 2004).

In Figure 2, there is a slight discrepancy between the observed intensities and model predictions for the CH_3OH lines at 151.86 GHz. The model predicts a higher line intensity than observed and underestimates the line intensity at 148.11 and 145.76 GHz. However, given the S/N of all the passbands where these lines are observed, the model does a very good job of predicting the expected line intensity of each CH_3OH transition observed with the 12 m telescope. The same can be said for the array data. The only discrepancy is the 96.7445 GHz $J(K_a, K_c) = 2(0,2)$–$1(0,1)$ E CH_3OH transition (Fig. 1); the intensity is somewhat underestimated by our model fit.

Figure 4 shows the best model fit to the $J(K) = 8(K)$–$7(K)$ ($K = 0$–6) transitions of methyl cyanide (CH_3CN) toward Comet Hale-Bopp. Once again, the blue line shows the model predictions for the CH_3CN data which are best fit by an excitation temperature of $T_{\rm ex} = 200 \pm 10$ K and a total beam-averaged column density of $N_T = (2.6 \pm 0.3) \times 10^{12}$ cm^{-2}. In this case, the predicted $K = 7$ line intensity is below the 1 σ detection limit, which indicates that the emission feature near the $K = 7$ rest frequency may not be real. Assuming a nuclear origin for CH_3CN and using a Monte Carlo model, we find a production rate of $Q(CH_3CN) \sim 1.7 \times 10^{27}$ s^{-1} or $Q(CH_3CN)/Q(H_2O) \sim 0.017\%$ at $\sim$1 AU. This production rate is similar to what Biver et al. (1997) found, $\sim 10^{27}$ s^{-1} at 1 AU, in their study.

These 12 m data overlap in frequency with the $(CH_2OH)_2$ IRAM 30 m study of Crovisier et al. (2004). In the IRAM data set, the claimed detection of the $J(K_a, K_c, v) = 15(7,9,0)$–$14(7,8,1)$ and 15(7,8,0)–14(7,7,1) transitions at 147.13 GHz are nearly coincident in frequency and show up as one feature given the spectral resolution. Moreover, the $(CH_2OH)_2$ transitions have an overall line intensity equal to that of the $J(K) = 8(4)$–$7(4)$ transition of CH_3CN detected with the IRAM 30 m telescope. From the ARO 12 m data, we identify the same spectral features of CH_3CN but do not detect any emission from the two transitions of $(CH_2OH)_2$ below the 1 σ limit. From the CH_3CN, CH_3OH, and $(CH_2OH)_2$ 12 m data, it is clear we are probing different physical environments in the coma of Comet Hale-Bopp. A discussion of the distribution of these molecular species is in § 4.2.

Figure 3 shows the best model fit (*blue line*) to the cluster of E-type transitions of CH_3OH centered around 157.26 GHz toward Comet LINEAR with the ARO 12 m telescope. There have been very few molecular line observations toward Comet LINEAR. The most complete study of molecular species toward this object was by Remijan et al. (2006) using the BIMA array. These authors detected the $J(K_a, K_c) = 3(1,3)$–$4(0,4)$ A^+ transition of CH_3OH with a synthesized beam size of $22.3'' \times 16.9''$. Using the proposed excitation temperature of 115 K (DiSanti et al. 2004; Magee-Sauer et al. 1999; Küppers et al. 2004), Remijan et al. determined a total beam-averaged column density for CH_3OH of $N_T = (1.4 \pm 0.3) \times 10^{14}$ cm^{-2}. However, as shown in Figure 3, the 12 m CH_3OH data are best fit by an excitation temperature of

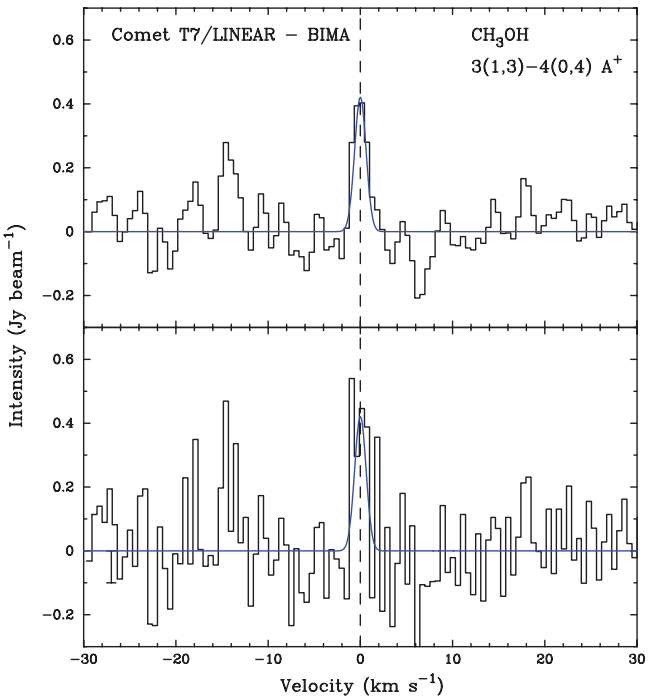

FIG. 5.—CH_3OH transitions from Comet LINEAR and the model fit to the data (*blue lines*) from the BIMA array data. *Top*: Hanning-smoothed data. *Bottom*: Raw data. See text.

$T_{ex} = 35 \pm 5$ K and a total beam-averaged column density of $N_T = (2.2 \pm 0.3) \times 10^{13}$ cm^{-2} (*blue line*), implying a production rate of $Q(CH_3OH) \sim 2.0 \times 10^{27}$ s^{-1} or $Q(CH_3OH)/Q(H_2O) \sim 1.5\%$ at 0.3 AU. This production rate ratio assumes $Q(H_2O) = 1.3 \times 10^{29}$ s^{-1} (Lecacheux et al. 2004). To reconcile the differing column density determined by Remijan et al. (2006), we used the best model fit parameters of temperature and column density from the 12 m data to predict the line intensity of the $J(K_a, K_c) = 3(1,3)$–$4(0,4)$ A^+ transition detected by the BIMA array. Figure 5 shows the result of this analysis (the top panel shows the Hanning-smoothed data, and the bottom panel shows the raw data as in Fig. 1 of Remijan et al. [2006]). The fit is excellent. From using the ARO data it is quite clear that the assumption of an excitation temperature of $T_{ex} = 115$ K for CH_3OH was incorrect, and the determined column density of CH_3OH toward Comet LINEAR was therefore overestimated by almost an order of magnitude.

4.2. *Distribution of Molecular Species*

We present two complementary sets of data from Comet Hale-Bopp that give great insights into the distribution of CH_3OH, CH_3CN, and $(CH_2OH)_2$. First, it is quite clear from the data presented in Figures 1 and 2 that despite the drastic change in the telescope beam sizes between the array and the 12 m telescope, we are still sampling a region of the coma that is thermalized to ~105 K. The ratio of areas subtended by the 12 m beam compared to the BIMA array synthesized beam is ~21:1, which corresponds to a change in the physical sampled size scale from $D \sim 40{,}000$ to 8500 km. A direct comparison of the column densities from the 12 m telescope and BIMA array suggest an enhancement of the CH_3OH abundance at smaller coma radii. Furthermore, column (5) in Table 3 lists the Einstein A-coefficients for each transition of CH_3OH, CH_3CN, and $(CH_2OH)_2$. Assuming a collision cross section of $\sim 10^{-15}$ cm^2 and a temperature of 105 K, the calculated critical densities of the detected CH_3OH transitions are in the range $(0.7$–$3.2) \times 10^5$ cm^{-3}. Our observations encompass a region with a H_2O density of $\sim 10^{(5.7-7.5)}$ cm^{-3} (Lovell et al. 2004). Therefore, there is sufficient collisional excitation to populate the CH_3OH levels, and our observations sample molecular abundances and not excitation effects.

Figure 6*a* once again shows the distribution of the $J(K_a, K_c) = 3(1,3)$–$4(0,4)$ A^+ transition of CH_3OH around Comet Hale-Bopp. Figure 6*b* is a model fit to the data shown in Figure 6*a*. The model was generated assuming a spherical Haser model of parent species sublimating off the comet's nucleus. From the data in Figure 6*a*, the scale length of the distribution of CH_3OH around the nucleus is measured to be $r \sim 10''$. Using this scale length and the MIRIAD task IMGEN, a Haser model distribution of CH_3OH was generated, which was then convolved with the synthesized beam of the BIMA array (Fig. 6, *bottom left of each panel*). The residuals obtained by subtracting the model from the data are shown in Figure 6*c*. While it appears that there may be a more extended distribution of CH_3OH detected by the BIMA array based on the residual data, it is important to note that the

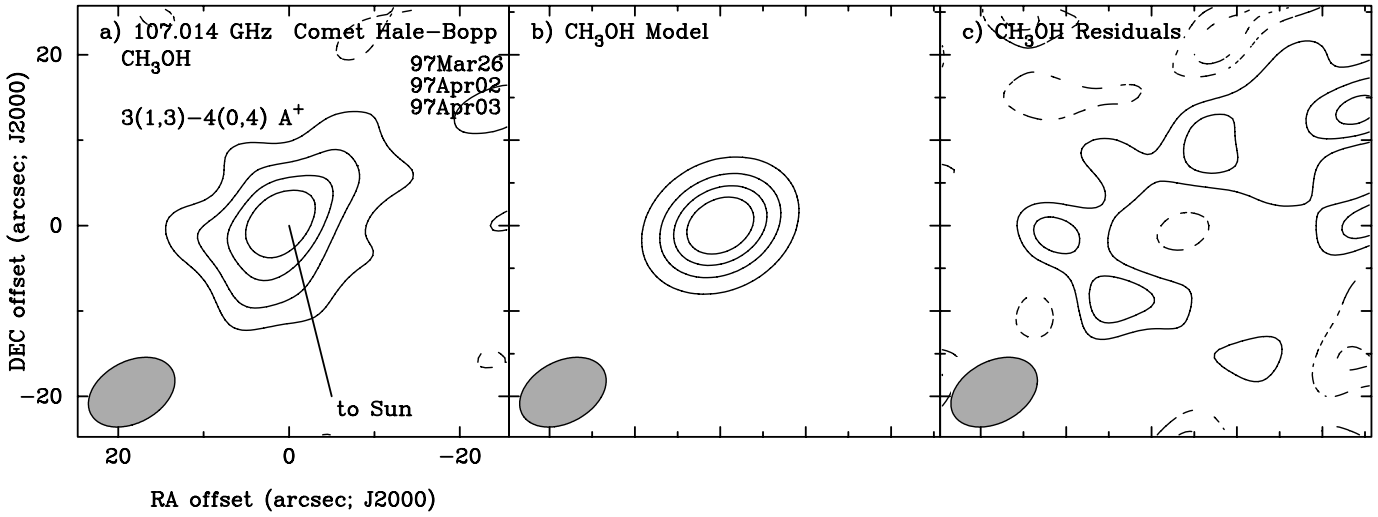

FIG. 6.—CH_3OH Haser model fit to the BIMA array data. (*a*) Emission contours from the 3(1,3)–4(0,4) A^+ transition of CH_3OH at 107.014 GHz. (*b*) Haser model predictions of these data assuming a scale length of $r \sim 10''$ and then convolved with the synthesized beam (*bottom left*). (*c*) Residuals obtained by subtracting the model from the data.

contour levels shown in Figures 6*a* and 6*b* are 3, 4, 5, and 6 σ ($\sigma = 0.05$ Jy beam^{-1}), whereas the data shown in Figure 6*c* are 1 and 1.5 σ. Although there is some indirect evidence for an extended distribution of CH_3OH with $D = 40,000$ km from the 12 m detections of CH_3OH, the data presented in Figure 6*c* indicate that any extended emission is completely resolved out by the array. The array would be sensitive to extended emission of CH_3OH in the outer coma only if the distribution were "clumpy," as is seen in H_2CO (Milam et al. 2006).

It appears that CH_3CN is tracing higher temperature and higher density gas than CH_3OH. Because CH_3CN has a larger dipole moment than CH_3OH, its measured excitation should be lower, given identical conditions. However, if the overall distribution of CH_3CN is closer to the nucleus than CH_3OH, we would expect to measure a higher excitation temperature (it is well known that the temperature of the coma increases with decreasing coma radii; Biver et al. 1999). This distribution would also imply that CH_3CN is a parent species (§ 4.3). Given the difference in beam sizes between the 12 and 30 m telescopes, we can get an estimate of the size of the emitting region based on the relative beam sizes using the beam filling factor in the expression for column density. Comparing the relative line intensities between the $K = 3$ and 4 transitions of CH_3CN from the IRAM 30 m data and what is measured from the 12 m telescope, the 30 m emission features from CH_3CN are ~5–10 times stronger than what is observed from the 12 m telescope. This difference implies either (1) an enhancement of the CH_3CN column density at smaller coma radii or (2) that the excitation of the transitions we observed of CH_3CN takes place at a slightly smaller radius, where the density is higher, and the measurements taken with the 12 m telescope are suffering from some beam dilution. Assuming the H_2O density profile of Lovell et al. (2004), the maximum coma radius that lies below the CH_3CN critical density range of $(1.2–5.3) \times 10^6$ cm^{-3} is ~10,000 km. This explains why the 30 m CH_3CN line strengths are higher than the 12 m. Finally, from the nondetection of $(CH_2OH)_2$ in the 12 m observations, it is also apparent that the distribution of $(CH_2OH)_2$ must also be compact in the cometary coma. Assuming that the detected transition line strength of ~0.09 K in the 30 m spectrum is from $(CH_2OH)_2$ and a 1 σ line intensity of ~0.01 K in the 12 m passband, the emission from $(CH_2OH)_2$ must be on the order of $D < 9''$, corresponding to a physical size of $D < 8500$ km. High-sensitivity, high-resolution interferometer observations are necessary to confirm this distribution.

4.3. *Formation of Cometary Methanol and Other Molecular Species*

From the high-resolution methanol observations of the BIMA array, it is clear that CH_3OH is either sublimating directly off the cometary ices contained in the nucleus or is formed very deep in the cometary coma. If CH_3OH originates in the ices, this molecule may be a remnant of the formation of the presolar nebula and hence the interstellar medium. Currently, there are two accepted formation pathways to the interstellar production of CH_3OH, including the radiative association of $CH_3^+ + H_2O \rightarrow CH_3OH_2^+$, followed by recombination with an electron to produce CH_3OH and H (Herbst 1985). Grain surface reactions that involve the repeated hydrogenation of $CO \rightarrow H + CO \rightarrow HCO + H \rightarrow HCHO \rightarrow HCHOH$ are thought to eventually lead to CH_3OH (Hiraoka et al. 1994). Our observations show that there is no significant enhancement in the production of CH_3OH in the outer coma as the comet enters the inner solar system.

The same argument can be applied to CH_3CN. The accepted route to the formation of CH_3CN in interstellar environments is $CH_3^+ + HCN$. A collision complex is formed that equilibrates to $CH_3CNH^+ + \nu$ (Herbst 1985), then CH_3CNH^+ combines with an electron to form $CH_3CN + H$. Our observations of CH_3CN show that it is currently close to the cometary nucleus, indicating direct sublimation off cometary ices. However, the excitation of the transitions we observed of CH_3CN takes place at a smaller radius where the density is higher, and this molecule may be present as well at larger radii. However, the true spatial scale and scale length of CH_3CN need to be verified by interferometric observations.

Finally, the nondetection of $(CH_2OH)_2$ with the ARO 12 m telescope gives insight into the formation of $(CH_2OH)_2$, as well as the possibility of detecting CH_2OHCHO. If the transition detected by the 30 m telescope is indeed from cometary $(CH_2OH)_2$, in § 4.2, we found that the predicted distribution of $(CH_2OH)_2$ toward Comet Hale-Bopp was calculated to be $D < 9''$ (<8500 km), again suggesting direct sublimation off cometary ices or enhanced production in the inner coma. Presumably, as with the formation of CH_3OH and CH_3CN in interstellar environments, $(CH_2OH)_2$ would be formed in the interstellar medium and then seeded into cometary ices. Currently, there is no accepted gas-phase interstellar formation mechanism that can lead to the production of $(CH_2OH)_2$. However, there are several formation pathways using surface chemistry which may occur on icy grain mantles. For example, to form $(CH_2OH)_2$ and CH_2OHCHO, formaldehyde (H_2CO) produces CH_2OHCHO in an aqueous Formose reaction, which can then be hydrogenated to form $(CH_2OH)_2$ (e.g., see Walker 1975). Charnley (2001) predicts that $(CH_2OH)_2$ and CH_2OHCHO could be formed by direct hydrogenation reactions, starting from ketene (CH_2CO) on grain surfaces. Finally, Hudson & Moore (2000) show that proton-irradiated CH_3OH on icy interstellar grain mantles can lead to the formation of $(CH_2OH)_2$. Thus, there appear to be several ways to form and embed $(CH_2OH)_2$ into cometary ices.

5. CONCLUSIONS

We present an interferometric and single-dish study of cometary molecules toward comets C/1995 O1 (Hale-Bopp) and C/2002 T7 (LINEAR) using the Berkeley-Illinois-Maryland Association (BIMA) interferometer at 3 mm and the Arizona Radio Observatory (ARO) 12 m telescope at 2 mm. The overall conclusions from our analysis of these data are as follows:

1. The CH_3OH Hale-Bopp data are well fit by an excitation temperature of $T_{ex} = 105 \pm 5$ K and a total beam-averaged column density of $N_T = (5.7 \pm 0.7) \times 10^{14}$ cm^{-2}. Assuming a nuclear origin for CH_3OH and using a Monte Carlo model, we find an average CH_3OH production rate from both instruments of $Q(CH_3OH) \sim 1.3 \times 10^{29}$ s^{-1} or $Q(CH_3OH)/Q(H_2O) \sim 1.3\%$ at ~1 AU.

2. The CH_3OH ARO 12 m LINEAR data centered around 157.26 GHz are best fit by an excitation temperature of $T_{ex} = 35 \pm 5$ K and a total beam-averaged column density of $N_T = (2.2 \pm 0.3) \times 10^{13}$ cm^{-2} and thus a production rate of $Q(CH_3OH) \sim 2.0 \times 10^{27}$ s^{-1} or $Q(CH_3OH)/Q(H_2O) = 1.5\%$ at 0.3 AU.

3. From the combination of the single-dish and aperture synthesis observations of CH_3OH, we find that the distribution of CH_3OH toward Comet Hale-Bopp is well described by a spherical outflow with an increase in column density closer to the cometary nucleus. The data presented in the array images show no evidence of significant enhanced production of CH_3OH in the extended coma or from jets, as any extended emission is completely resolved out by the array.

4. The CH_3CN 12 m Hale-Bopp data are best fit by an excitation temperature of $T_{ex} = 200 \pm 10$ K and a total beam-averaged column density of $N_T = (2.6 \pm 0.3) \times 10^{12}$ cm^{-2}. Assuming a nuclear origin for CH_3CN and using a Monte Carlo model, we find an average CH_3CN production rate of $Q(CH_3CN) \sim 1.7 \times 10^{27}$ s^{-1} or $Q(CH_3CN)/Q(H_2O) \sim 0.017\%$ at $\sim$1 AU. A comparison between the single-dish observations from the ARO 12 m telescope and the IRAM 30 m telescope of CH_3CN suggest that the ARO observations are beam-diluted. The excitation of the observed transitions of CH_3CN takes place at a smaller radius where the density is higher and suggests a nuclear origin of CH_3CN.

5. The nondetection of a previously claimed transition of cometary $(CH_2OH)_2$ toward Comet Hale-Bopp with the ARO 12 m telescope indicates a compact distribution of emission on the order of $<9''$ ($<$8500 km). This supports the hypothesis that the cometary production of $(CH_2OH)_2$ is via direct sublimation off cometary ices from the nucleus.

We thank D. K. Yeomans for ephemerides assistance and G. Engargiola, T. Helfer, W. Hoffman, R. L. Plambeck, and M. W. Pound for invaluable technical contributions. We also thank an anonymous referee for a favorable review of this work and whose comments and suggestions provided additional clarity to this manuscript. This material is based on work supported by the National Aeronautics and Space Administration through the NASA Astrobiology Institute under Cooperative Agreement CAN-02-OSS-02 issued through the Office of Space Science. S. N. M. would like to thank the Phoenix Chapter of ARCS, specifically the Mrs. Scott L. Libby, Jr. endowment, for partial funding. This work was partially funded by NASA NAG5-4292, NAG5-4080, NAG5-8708, and NGT5-0083; NSF AST 96-13998, AST 96-13999, AST 96-13716, AST 96-15608, and AST 99-81363; and the Universities of Illinois, Maryland, and California, Berkeley. M. W. was funded by NSF AST 96-25360, AST 97-96263, and AST 00-98583 and NASA NAG5-4349.

REFERENCES

Araya, E., Hofner, P., Kurtz, S., Bronfman, L., & DeDeo, S. 2005, ApJS, 157, 279
Biver, N., et al. 1997, Earth Moon Planets, 78, 5
———. 1999, AJ, 118, 1850
———. 2002, Earth Moon Planets, 90, 5
Bockelée-Morvan, D., Crovisier, J., Despois, D., Forveille, T., Gerard, E., Schraml, J., & Thum, C. 1987, A&A, 180, 253
Bonev, B. P., Mumma, M. J., Radeva, Y. L., DiSanti, M. A., Gibb, E. L., & Villanueva, G. L. 2008, ApJ, 680, L61
Charnley, S. B. 2001, in The Bridge between the Big Bang and Biology, ed. F. Giovannelli (Rome: Consiglio Naz. Ric.), 139
Charnley, S. B., & Rodgers, S. D. 2008, Space Sci. Rev., 138, 59
Christen, D., & Müller, H. S. P. 2003, Phys. Chem. Chem. Phys., 5, 3600
Colom, P., Despois, D., Bockelée-Morvan, D., Crovisier, J., & Paubert, G. 1990, in Workshop on Observations of Recent Comets, ed. W. F. Huebner (San Antonio: Southwest Res. Inst.), 80
Combi, M. R., & Smyth, W. H. 1988, ApJ, 327, 1026
Crovisier, J., Bockelée-Morvan, D., Biver, N., Colom, P., Despois, D., & Lis, D. 2004, A&A, 418, L35
DiSanti, M. A., Reuter, D. C., Mumma, M. J., Dello Russo, N., Magee-Sauer, K., Gibb, E. L., Bonev, B., & Anderson, W. M. 2004, BAAS, 36, 1122
Herbst, E. 1985, ApJ, 291, 226
Hiraoka, K., Ohashi, N., Kihara, Y., Yamamoto, K., Sato, T., & Yamashita, A. 1994, Chem. Phys. Lett., 229, 408
Hofner, P., Kurtz, S., Churchwell, E., Walmsley, C. M., & Cesaroni, R. 1996, ApJ, 460, 359
Hudson, R. L., & Moore, M. H. 2000, Icarus, 145, 661
Hudson, R. L., Moore, M. H., & Cook, A. M. 2005, Adv. Space Res., 36, 184
Huebner, W. F., Keady, J. J., & Lyon, S. P. 1992, Ap&SS, 195, 1
Küppers, M., Hartogh, P., & Villanueva, G. 2004, BAAS 36, 1125
Lecacheux, A., Biver, N., Crovisier, J., & Bockelée-Morvan, D. 2004, IAU Circ. 8304
Lovell, A. J., Kallivayalil, N., Schloerb, F. P., Combi, M. R., Hansen, K. C., & Gombosi, T. I. 2004, ApJ, 613, 615
Magee-Sauer, K., Mumma, M. J., DiSanti, M. A., Russo, N. D., & Rettig, T. W. 1999, Icarus, 142, 498
Milam, S. N., et al. 2006, ApJ, 649, 1169
Müller, H. S. P., Schloder, F., Stutzki, J., & Winnewisser, G. 2005, J. Mol. Structure, 742, 215
Mumma, M. J., et al. 2003, Adv. Space Res., 31, 2563
Remijan, A., Sutton, E. C., Snyder, L. E., Friedel, D. N., Liu, S.-Y., & Pei, C.-C. 2004, ApJ, 606, 917
Remijan, A. J., et al. 2006, ApJ, 643, 567
———. 2007, BAAS, 39, 963
Sault, R. J., Teuben, P. J., & Wright, M. C. H. 1995, in ASP Conf. Ser. 77, Astronomical Data Analysis Software and Systems IV, ed. R. A. Shaw, H. E. Payne, & J. J. E. Hayes (San Francisco: ASP), 433
Snyder, L. E., et al. 2005, ApJ, 619, 914
Taylor, B. N., & Kuyatt, C. E. 1994, NIST Tech. Note 1297 (Washington: US GPO)
Veal, J. M., et al. 2000, AJ, 119, 1498
Walker, J. F. 1975, Formaldehyde (3rd ed.; Huntington: R. E. Krieger), chap. 8
Weissman, P. R. 1999, Space Sci. Rev., 90, 301